
mag □
8 796 x
30 µm
Earth Science, University of Manitoba

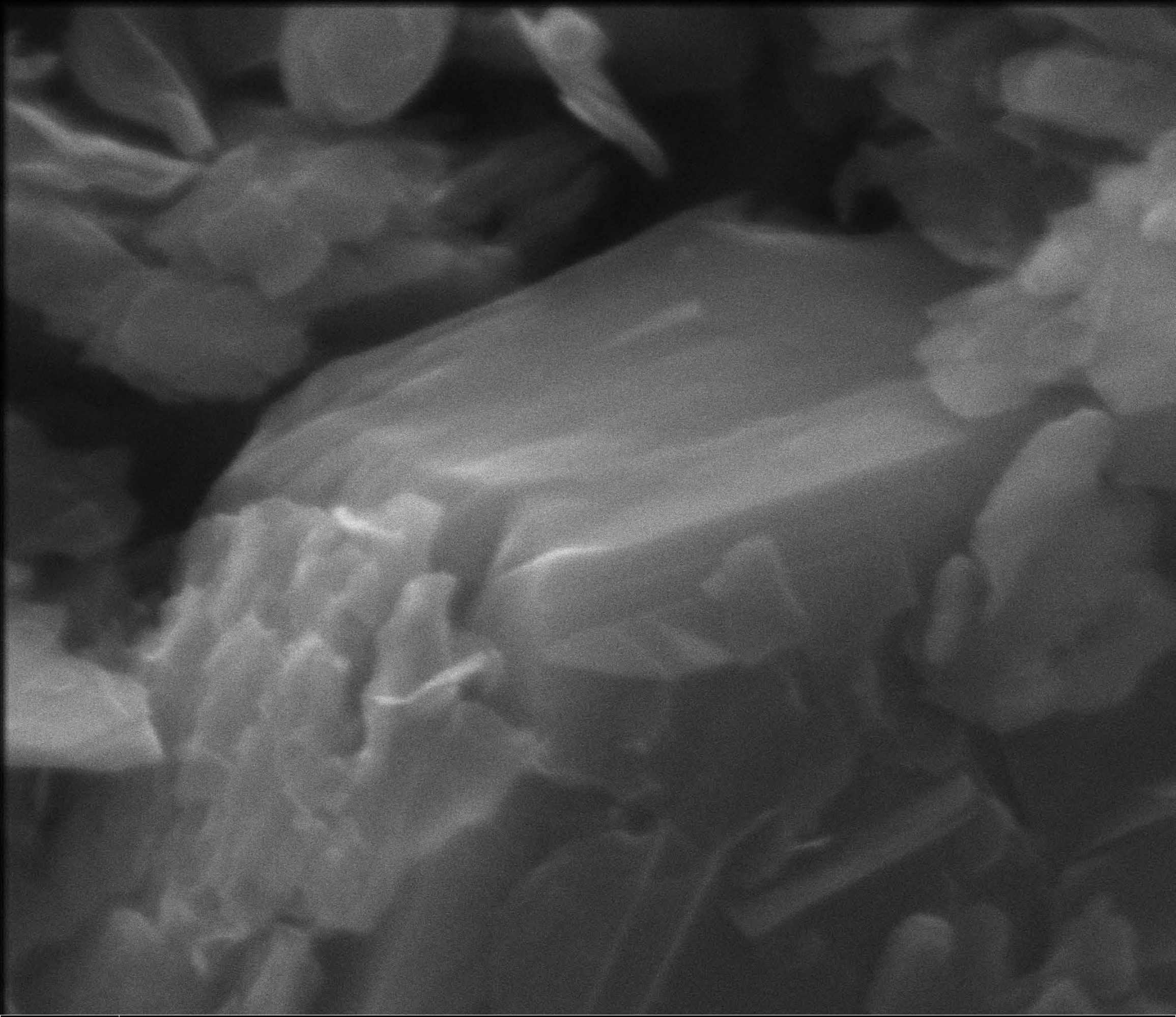
mag
83 678 x
3 µm
Earth Science, University of Manitoba

Major take aways:

- Feed solid consists of a mix of graphite, quartz, plagioclase, muscovite and chlorite. Graphite content, based on XRD, is in the range of 65-79 modal%.
- The three concentrate samples all yield high purity graphite. Graphite purity is estimated to be >98% due to absence of peaks from gangue minerals identified in the feed solid sample.
- Rockstone graphite consists of hexagonal graphite with turbostratic disordering.
- Graphite oxide appears to be present in all analyzed samples.
- Estimated graphitization temperatures are low (200-300°C), and may reflect structural modifications induced during beneficiation procedures.

Rockstone XRD Pattern Characteristics

XRD patterns for Rockstone concentrates (washed/unwashed residues) are similar and consistent with samples consisting of >98 modal% of hexagonal graphite with turbostratic disordering (Figs. 1 to 4). The peak positions for the (002) peak (Fig. 3) and the (100) peak at approximately 42.5°2θ (Fig. 4) are indicative of hexagonal graphite. The broad peak or "hump" from approximately 43 to 46°2θ (Fig. 4) is indicative of tubrostratic graphite.

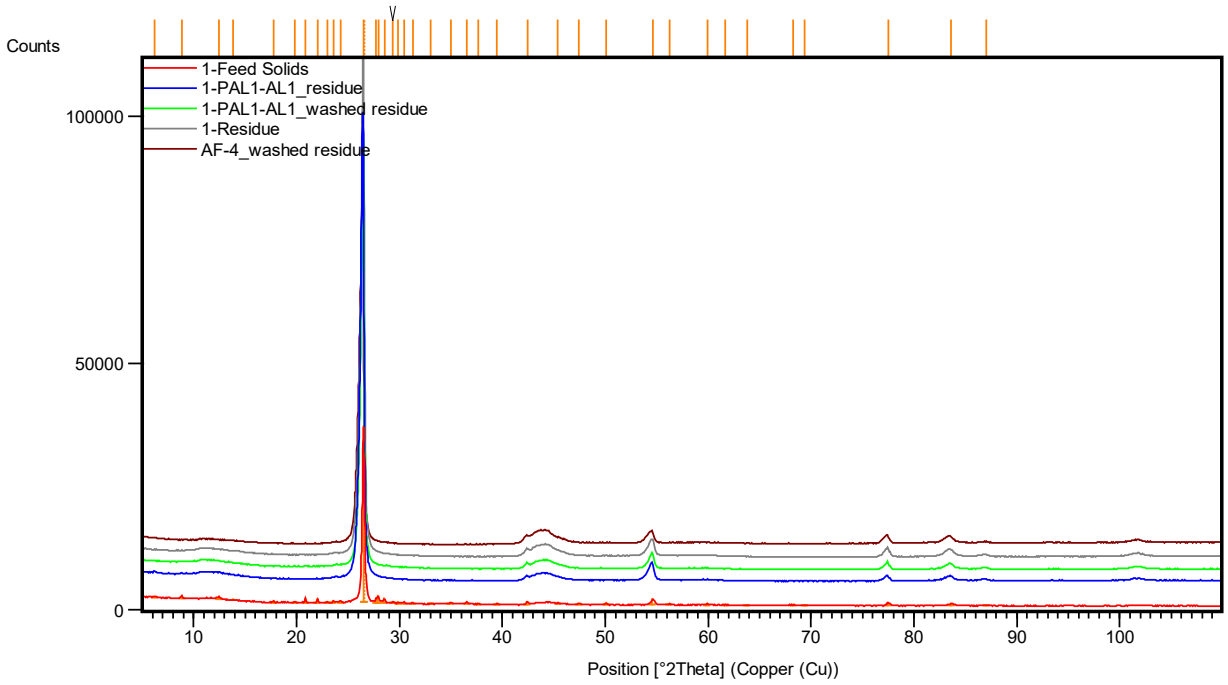

Figure 1. Comparative XRD patterns (full 2θ scan range) of Rockstone graphite feed and concentrates.

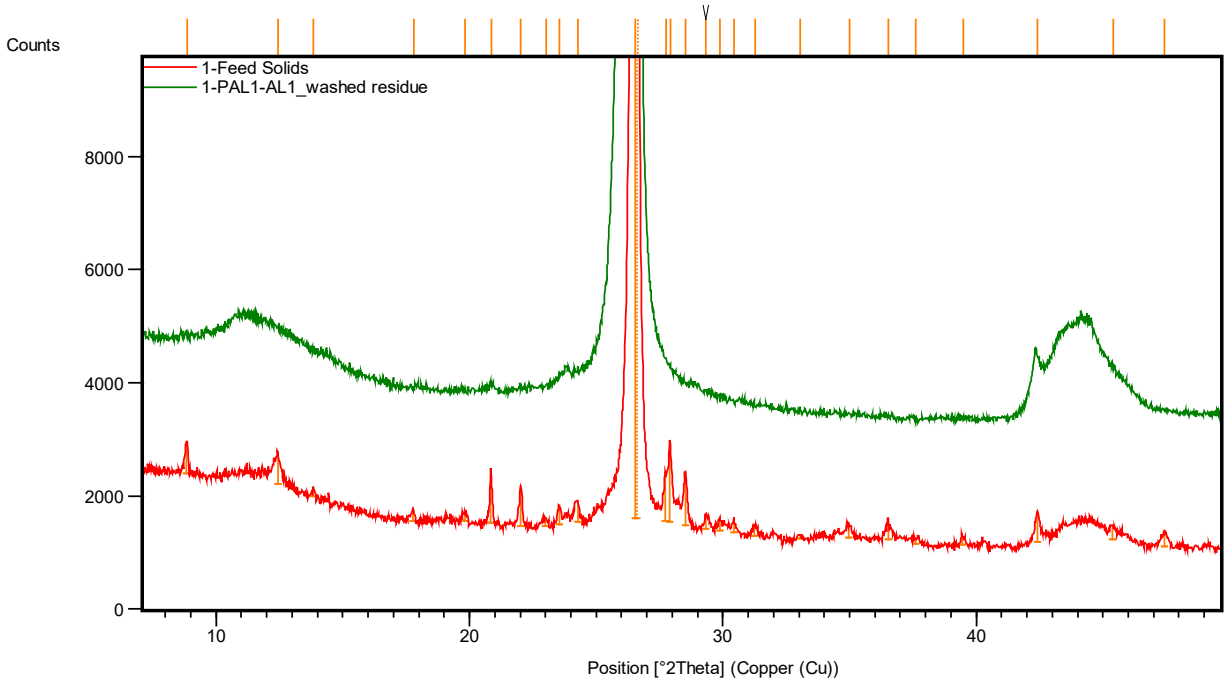

Figure 2. Rockstone feed and PAL1-AL1 washed residue concentrate. Note that the feed solids pattern is characterized by additional peaks, broadening/offset of the 002 peak and general lower intensity of graphite peaks indicating significant presences of additional mineral phases.

Figure 2 illustrates differences in the relative purity of the concentrates to the feed solids. The feed material is comprised of 65-79% graphite (depending on method of modal estimation) with the impurities consisting (in order of decreasing abundance) quartz, plagioclase feldspar, muscovite and chlorite. The relatively high abundance of quartz (xxx%) in the feed solids results in an overlap between the (002) peak of graphite and (101) peak of quartz, resulting in apparent shift to higher two-theta values. Consequently, it is not possible to obtain accurate crystallographic properties of Rockstone graphite from the feed sample, as the determination of key crystallographic attributes (i.e., L_a-L_c parameters) requires precise measurement of the FWHM of the (002) peak of graphite.

Figure 2 also illustrates the occurrence of a board peak that ranges from approximately 10 to 15°2θ and centred around 12°2θ. This peak corresponds to the development of graphite/graphene oxide likely reflects expanded turbostratic stacking nanographite. The general shape of this peak is consistent with experimental studies that suggest development under low to moderately low oxidizing conditions. In addition, the broadening and asymmetry of the (002) peak (Fig. 3) is also consistent with the development of turbostratic graphite and graphite oxide.

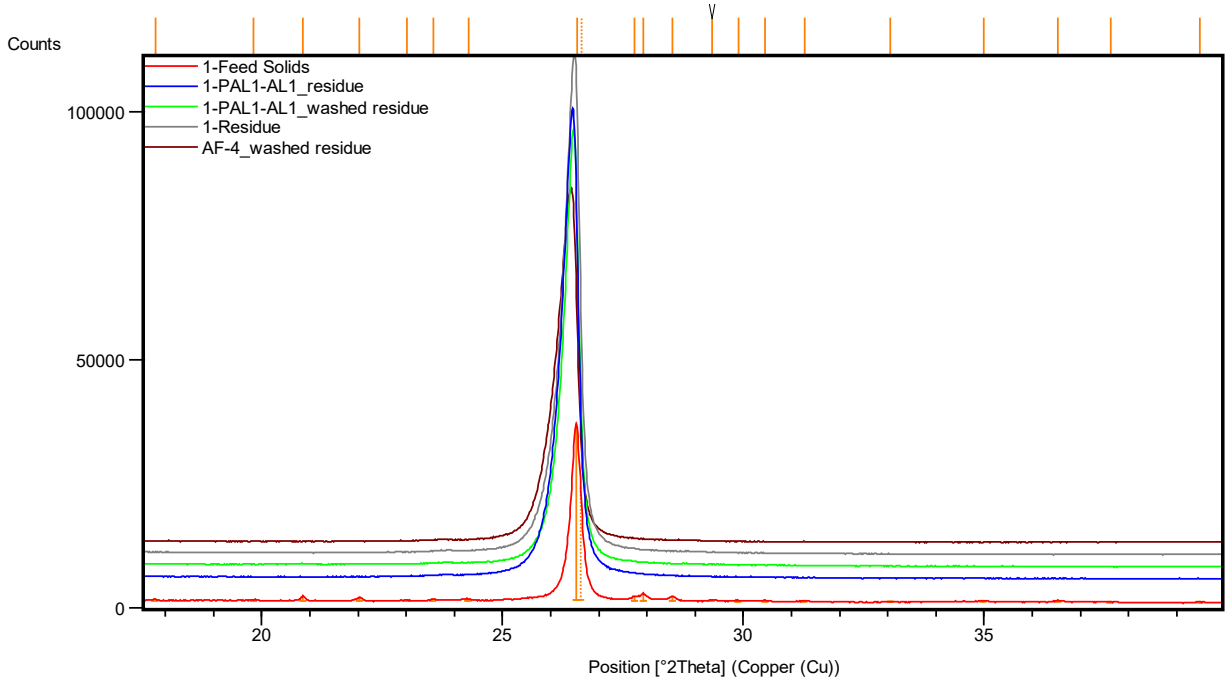

Figure 3. Comparative XRD patters of Rockstone graphite feed and concentrates for the (002) peak region (basal plane reflection).

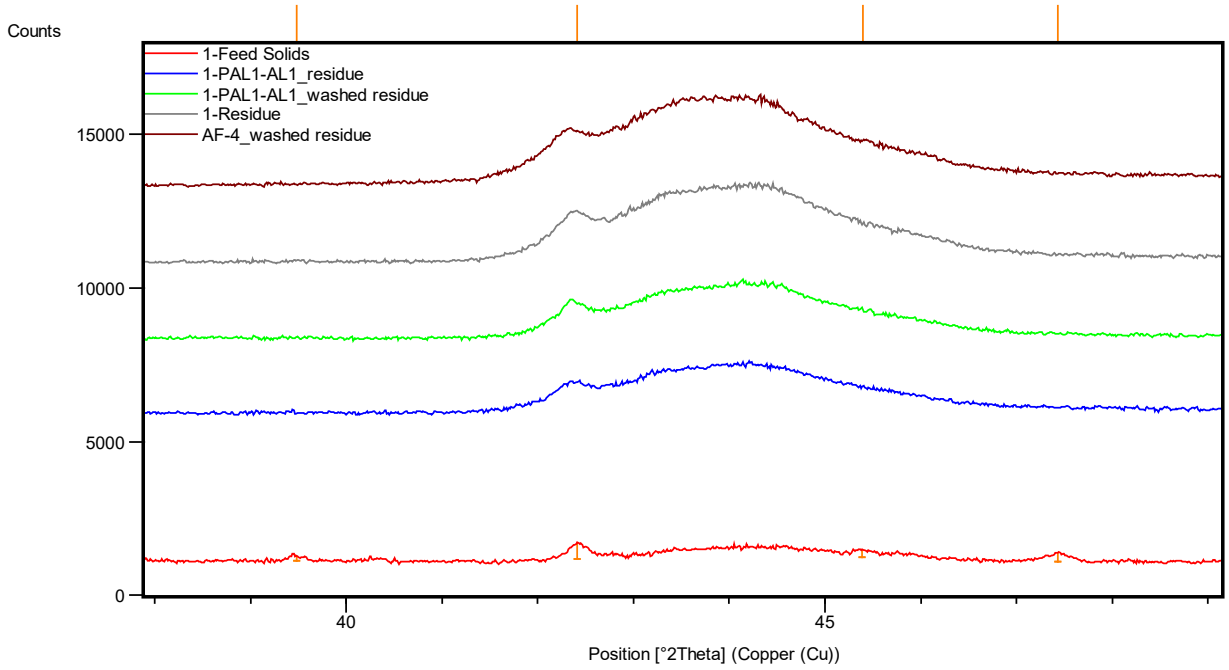

Figure 4. Comparative XRD of Rockstone graphite feed and concentrates for the prismatic region (41-46°2θ).

Comparative XRD

Figures 5 to 7 provides a comparison a XRD pattern of Rockstone concentrate to the patterns for the following:

- **Graphene oxide**: this is graphene oxide that is produced from a concentrate of natural hexagonal graphite.
- **CPREME-G8**: synthetic graphite produced by ConocoPhillips Co.
- **Bogala**: Natural, highly crystalline graphite form the Bogala mine, Sri Lanka.
- **Nat. Chinese**: This is natural hexagonal and rhombohedral graphite concentrate from China, which is used in the manufacturing of Li-ion batteries.

These samples were selected as they illustrate a diverse range of crystallographic features that are common to natural and synthetic graphite.

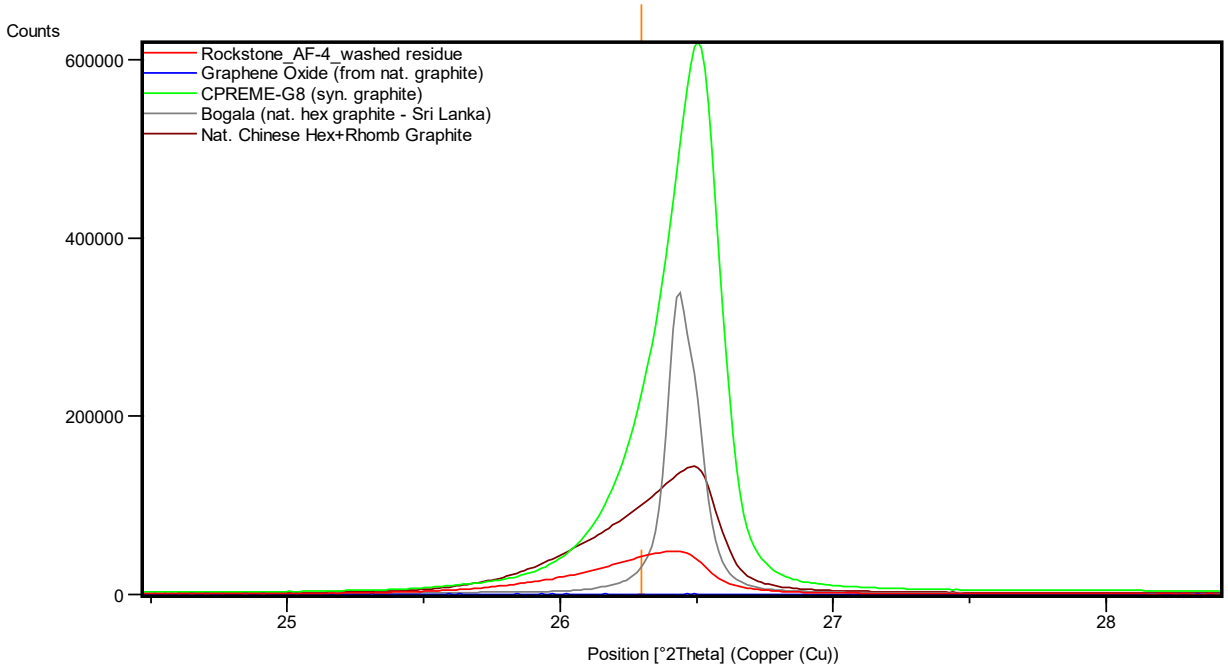

Figure 5. Comparative XRD patters of Rockstone graphite concentrates and other natural and synthetic graphite and graphene oxides samples for the (002) peak region.

The position of the (002) peak is a function of the d-spacing of the (002) plane, where shifts to higher °2θ reflect a decrease in the d-spacing. The (002) peak for hexagonal graphite does overlap with the (003) peak for rhombohedral graphite and the (101) peak for quartz. In terms of the samples illustrated in Figure 5, the near Gaussian (002) peak for CPREME-G8 is characteristic of hexagonal graphite. The (002) peak for Bogal, does display a minor asymmetry (a shoulder on the higher °2θ side), possible reflecting the inclusion of some quartz (as this sample was prepared from a large lump graphite sample). Graphene (including nano-graphite with less than 11 graphene layers) does not yield (002) peaks. Both Rockstone and the natural Chinese samples display moderate asymmetry, with a skew to lower °2θ. For

the Chinese sample, this reflects the presence of both hexagonal and rhombohedral graphite (also see Figure 6). On the other hand, the asymmetry of the (002) peak for Rockstone graphite reflects presence of turbostratic graphite.

The shape of the (002) peak, in particular broadening also reflects reduced grain/crystallite sizes. However, to access crystallite size parameters (L_a and L_c) it is necessary to dope highly pure samples with a silicon standard (see ongoing and future work).

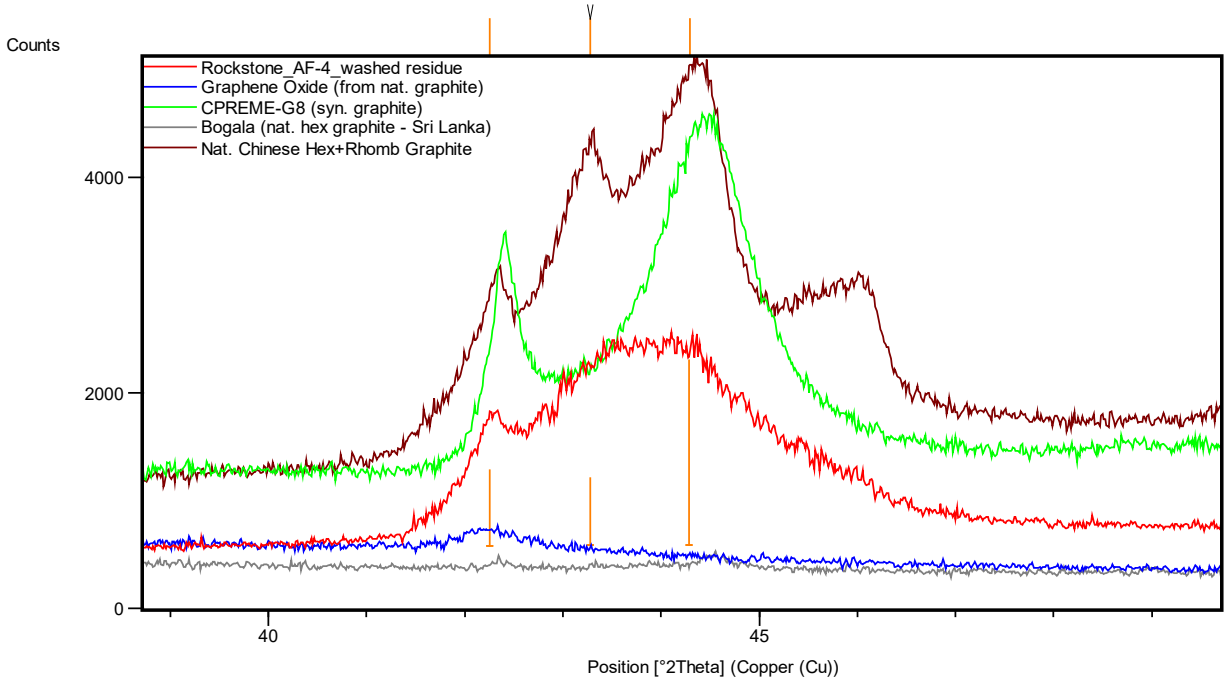

Figure 6. Comparative XRD patters of Rockstone graphite concentrates and other natural and synthetic graphite and graphene oxides samples concentrates for the prismatic region (41-46°2θ).

As previously stated, the differentiation among hexagonal, rhombohedral and turbostractic is most readily accomplished by identification of the peaks (representing edge reflections) that comprise the prismatic region of an XRD pattern (Fig. 6). Samples, such as CPREME-G8, that consist solely of highly crystalline, hexagonal graphite will only yield two peaks within this region. The hexagonal peaks correspond to (100) (at approximately 42.5°2θ) and (101) (at approximately 44.5-45°2θ). In contrast, a highly crystalline sample consisting of both hexagonal and rhombohedral graphite, such as the natural Chinese graphite sample, will yield four peaks within this region. Two of the peaks correspond to the (100) and (101) planes of hexagonal graphite, with the other two being generated by the (101) (at approximately 43.5°2θ) and (102) (at approximately 46-46.5°2θ) planes of rhombohedral graphite. Rockstone concentrates yield the characteristic pattern of hexagonal graphite with turbostractic modifications to the graphite structure. Turbostractic, hexagonal graphite typically yields a reflection from the hexagonal (100) plane and then a broad peak that extends over a two-theta range that is equal

to the angular range of other hexagonal and rhombohedral prismatic peaks. The XRD patterns for the graphene oxide sample and Bogal do not yield any clearly discernable peaks within the prismatic region. For graphene oxide sample there is a week peak in the same position of the (100) plane for hexagonal graphite; and this likely an edge induced reflection for a graphene oxide sample that does not consist of a single graphene nanosheet but is comprised of nano to micro graphene oxide (2-11 layers). The absence of any hexagonal prismatic plane reflections for Bogal is a product of sample preparation, where the sample was prepared on a zero-background plate by dropping a suspension of weakly milled graphite. This would have induced a preferred orientation, with graphite flakes being deposited so the basal plane is aligned parallel to the zero-background plate and resulted in a relative increase in the intensity of the (002) peak and corresponding decreases in the intensity of the prismatic peaks.

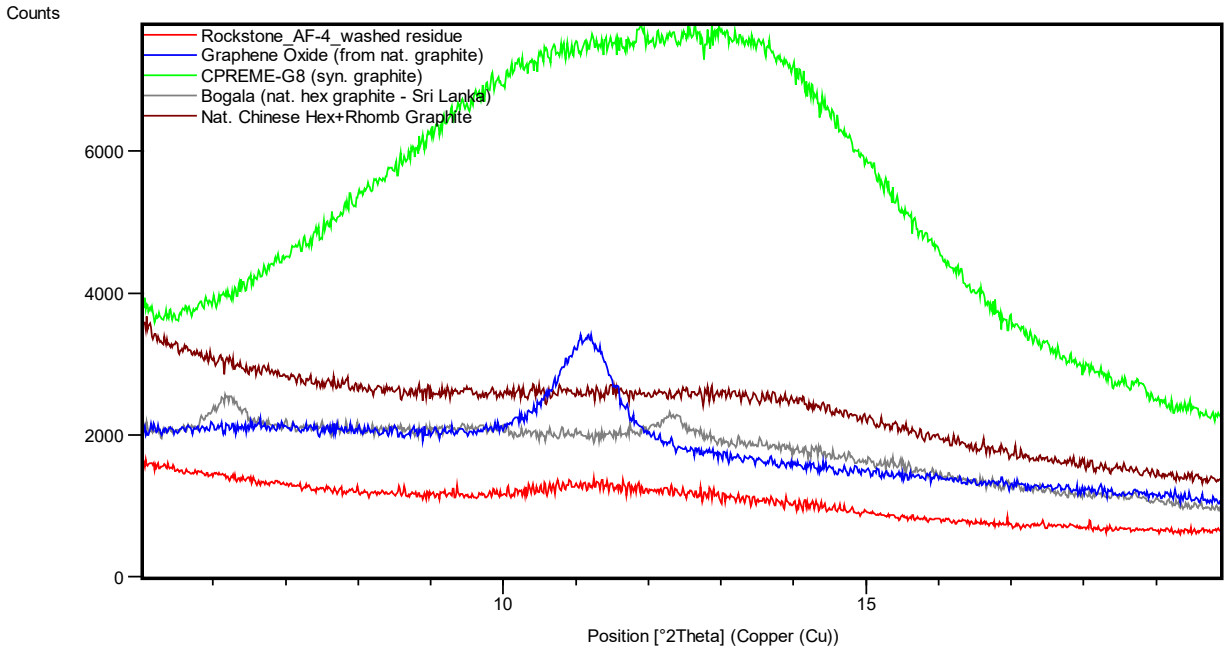

Figure 7. Comparative XRD patters of Rockstone graphite concentrates and other natural and synthetic graphite and graphene oxides samples concentrates for the low-angle region (5-20°2θ).

The low-angle region (5-20°2θ) is an important region of the identification of graphite, graphene oxide and graphite oxide (Fig. 7). It is important to note the Rockstone graphite yields significantly lower peak intensities than the other samples (as also the case for the (002) peak, Figure 5) in this region. Consequently, the broad peak that is readily observable in Figure 2 is much less pronounced in Figure 5. Difference in intensities can reflect differing operating parameters of the XRD instrument. However, all samples were analyzed under the same operating conditions. The nano- to micro-graphene oxide yield a well defined (002) peak that is centred around 11°2θ. However, graphite samples that contain a broad, relatively low intensity peak (Rockstone, CPREME-G8 and natural Chinese graphite) likely reflect the presence of graphite oxide and reduced graphite oxide. However, the presence of oxidized forms of

graphitic carbon will be confirm using silicon-doped samples run on a zero-background plate and various spectroscopic methods.

Preliminary Graphite Geothermometry

Determination of the temperature of graphitization was on conduct on the quartz-free concentrates using the graphite geothermometer of Shengelia et al. (1979). Temperatures are reported with errors of ±20°C and have not been corrected for possible instrument induced peak shifts.

Table 1: Summary of graphite geothermometry of Rockstone concentrate samples.

Sample No	°2θ	FWHM	d-spacing (002)	Temperature (°C)
PAL1-AL1 washed residue	26.3733	0.37540	3.3767	223.3
PAL1-AL1 residue	26.3909	0.38386	3.3745	270.8
Residue	26.3964	0.38924	3.3738	285.7
AF-4	26.2983	0.44452	3.3861	19.5

The temperature for AF-4 is clearly in error. This may reflect modification of the graphite structure during sample preparation. However, to be certain, this and all samples (excluding the Feed) will be reanalyzed by XRD using zero-background plates and doped with a silicon standard (which enables corrections of instrument induced peak shift).

Excluding AF-4, the other three samples do yield similar temperatures, though PAL1-AL1 washed residue is outstand of the ±1σ range of samples PAL1-AL1 residue and Residue. Regardless of any statistical differences, the three samples all yield very low graphitization temperatures. The graphite geothermometer of Shengelia et al. (1979) is calibrated for a temperature range of 200 to 900°C. The estimate temperatures for the Rockstone samples are below the lower temperature limit for regional metamorphism associated with greenschist rocks (the host rocks do appear to be consistent with greenschist facies). Determination of the grade of metamorphism of the host rocks is required. Nonetheless, the low graphitization temperatures may reflect structural modifications induced during the preparation of the concentrates.

Ongoing and Future work

X-ray Diffraction

The next round of XRD on the provided concentrate samples will be done on silicon-doped samples and use a zero-background plate. This approach will enable correction of peak positions induced by the instrument. These results will also provide revised temperature estimates and key crystallite size parameters (L_a and L_c).

XRD work will also be conducted on graphite extracted from drill core, to constrain the inherent properties. Owing that quartz-free samples are required, any extracted graphite will require a limited degree of purification, which may induce structural modifications. *In situ*, small area XRD will be attempted. However, the fact that Rockstone graphite is intergrown with quartz, may limit the usefulness of *in situ* XRD. This data will eventually be compared to *in situ* spectroscopic investigations being conducted as part of the MSc study at the University of Manitoba.

Electron Microscopy

Preliminary electron microscopy has been done. Additional work may be conducted if determined necessary.

Spectroscopic Analyses

This will include an integration of Fourier Transform Infrared Spectroscopy (FTIR), micro-Raman spectroscopy (μRaman) and X-ray photoelectron spectroscopy (XPS). μRaman of concentrates will be conducted to further confirm structural modifications identified by XRD and possibly further constrain temperature estimations. *In situ* Raman of polished sections of drill core will form part of the MSc student underway at the University of Manitoba. FTIR and XPS analyses will be conducted to characterize the oxidized forms of graphite in the concentrates.

Comparison to unprocessed Rockstone graphite

This will require careful separation and minimal preparation (to ensure minimal quartz contamination) of Rockstone graphite from core samples. Initial work will consist of XRD analyses, and pending on those results, may progress to include electron microscopy and spectroscopic analysis.

Interpretation

The turbostractic graphite and graphite/graphene oxide associated with Rockstone graphite is likely a product of the processing. As both these features are present in the feed and concentrate samples. However, to confirm this, will require comparison with unprocessed Rockstone graphite.